TOWARD SEMI-AUTONOMOUS PROSTHETIC HAND CONTROL: APPLYING EMBEDDED NEURAL NETWORKS TO IMPROVE SENSOR FUSION IN PROSTHETIC FINGERTIP SENSORS

[1]Ben Pulver, [2]Sarah Aguasvivas Manzano, [2]Aaron Selnick, [1]Serena Kishek, [1]Levin Sliker, [2]Nikolaus Correll, [2]Jacob Segil

[1]Point Designs LLC, [2]University of Colorado Boulder

ABSTRACT

We present an application of embedded, real-time neural network predictions to produce reliable sensing and enable semi-autonomous control of a prosthetic hand with embedded tactile sensors at the fingertips. We simultaneously predict the force magnitude and the position of contact, requiring on average 32.8ms, thereby enabling real-time measurements. We demonstrate 97.2% offline classification accuracy on the contact position, and a root mean squared error of 1.38 N (mean absolute error of 0.68 N) in predicting the force magnitude. Neural networking training is performed off-line on a Desktop computer using Keras and compiled into efficient C-code for a nrf52840 microcontroller using the open-source tool "nn4mc." The training model, as well as the nn4mc compiler, are available online, allowing prosthetic engineers to incorporate real-time, sensor-based inference into their prosthetic design.

INTRODUCTION

Approximately 60,000 people live with major upper-limb amputations in the United States [1]. Many individuals opt to use a prosthetic device to restore some level of functionality. A variety of myoelectric prosthetic hands are now available, including multi-functional devices that can achieve different grasp patterns [2]. However, without sensory feedback, these advanced devices are lacking compared to intact limbs. This is why older technologies like body-powered devices, which do provide some sensory feedback, continue to be commonly used [3].

Adding sensory feedback to myoelectric devices can allow for semi-autonomous control, where the control is shared between the human and the device [4]–[6]. Prior methods relied on data that occurred after contact with an object [7]–[9] or extrinsic camera systems [6]. The Point Touch fingertip sensors enable three-phased control which depends on where the prosthetic device is relative to a nearby object. Myoelectric control systems are used for direct volitional control of the hand. Then, autonomous functions pre-contact and post-contact are enabled using proximity and force detection within the fingertip sensors. This future effort will be built upon the developments presented here.

Amputees can benefit from receiving haptic feedback on the localization of contact in order to obtain finer contextual information on the grasping task being performed [10]. Here, we present current developments on onboard neural network predictions with the help of the *nn4mc* compiler[1][11]. We simultaneously predict force magnitude and region of contact at the fingertip based on barometric and infrared sensor signals. The model used for prediction is embedded into the microcontroller that collects sensor data. This eliminates overhead in communication, increases the safety and security of the user's raw sensor data, and enables prosthetic engineers and designers to embed advanced predictions that can be computed at lower latencies.

BACKGROUND

The Point Touch is a novel multimodal tactile sensor that consists of an infrared proximity sensor and a barometric pressure sensor embedded in an elastomer layer [12]. Signals from both sensors measure proximity (0-10 mm), contact (0 N), and force (0-50N) which can be utilized in a variety of ways. The barometer provides a reliable force measurement for neural interfaces when restoring the sense of touch [12]. The proximity sensor presents a new possibility of using prosthetic fingers to "see" the world around them.

[1] https://nn4mc.com

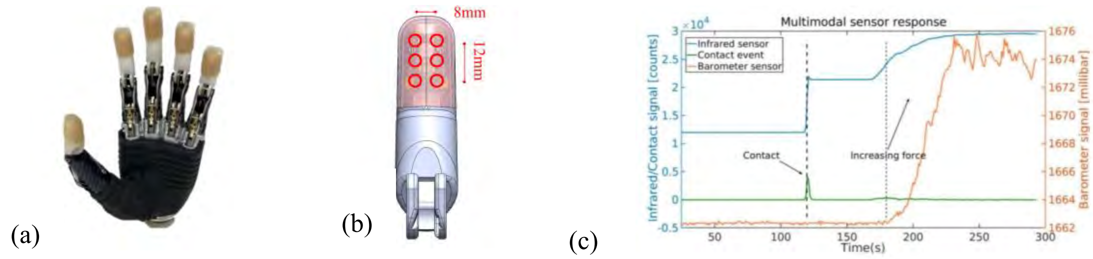

Figure 1: (a) The Point Touch integrated into the Bebionic hand. (b) High-level sensor architecture (c) Sensor response when a small piece of cotton is dropped onto the sensor and pressed.

MATERIALS AND METHODS

Experimental Procedure

Our approach consists of three steps: data collection, neural network training, and deployment of the neural network model on a microcontroller that collects sensor signals from the fingertip.

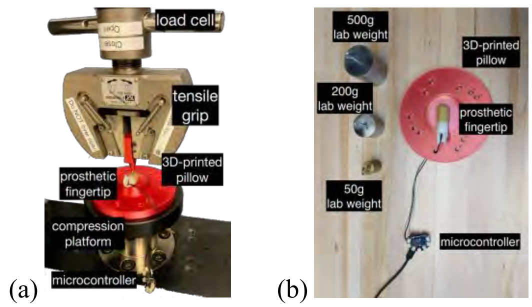

Figure 2: (a) Data collection setup using a universal test machine and a custom-made pillow for the fingertip sensor. (b) Experimental setup to collect real-time prediction results from the fingertip.

We collect force data and sensor signal data from a universal testing machine (UTM) (Universal Testing Machine, MTS Systems). A custom compression test up to 50N is conducted via positional control of the UTM (see Figure 2a). We zero the position of the tip of the UTM when mild contact occurs with the surface of the fingertip elastomeric material. The material is met with a 5mm externally threaded surgical steel ball (Steel Balls, Prjndjw Jewelry). Then, the force is recorded at the PC (Instron TW Elite on Windows) that controls the UTM machine and the barometric and infrared sensor data is collected directly from the fingertip board. Figure 2b displays the experimental setup to collect real-time results. A set of three dead weights where each mass is placed in a direction normal to the fingertip sensor area. Figures 4a–4e are extracted using the experimental setup in Figure 2b.

Algorithm Design and Implementation

We keep a window of 30 data samples at a time. This window behaves like a double-ended queue (deque): when each of the fingertip samples is collected for both barometric and infrared sensor data, the front of the deque is pushed with the most recent sensor data samples, whereas the last sample in the window is deleted.

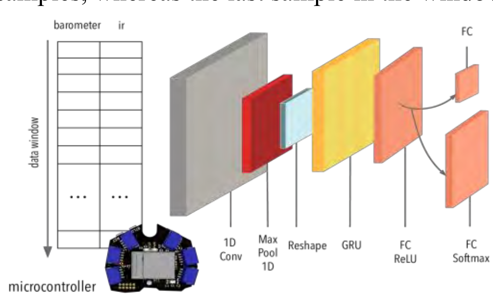

Figure 3: Neural network model; the architecture is interpreted from left to right.

The neural network model begins with a 1-dimensional convolutional layer with 16 filters and a kernel of size 2. We add a 1-dimensional max-pooling layer with a pool size of 3 and 3 strides. The output is then reshaped into a row vector. A gated recurrent unit (GRU) of 20 units of output takes the row vector and feeds its output to a fully-connected

(FC) layer with a rectified linear unit (ReLU) that outputs 10 units. The output of this layer is copied into two other FC layers: a one-neuron-wide FC hyperbolic tangent layer that outputs the normalized values for force and a 6-unit-wide FC layer with a softmax activation function that outputs the probability density function of the region of touch. The neural architecture is shown in Figure 3. The GRU is needed to trace temporal information through the recurrent layer's internal memory [13]. The output of this neural network is a 7-element vector $\boldsymbol{v} = \{v_0, v_1, \dots, v_6\}$, where each value is between -1 and 1. This is then mapped back into force in Newtons and elements $\{v_1, \dots, v_6\}$ indicate values between 0 and 1. Here, $v_i = 0$ indicates a value of l of the region i having any external contact and $v_i = 1$ means a high likelihood of the region i having any force applied to it.

For training, a 5-fold time series is split and each split trains using a batch size of 50 samples and for 20 epochs. The offline testing set results for location of contact are displayed in Figure 4a. We use a mean-squared-error loss for the part of the neural network that is learning normalized force magnitude and a categorical cross-entropy loss for the part of the neural network that is predicting the localization of contact.

The deployment of the neural network into the microcontroller is done through *nn4mc* [11], an open-source compiler that generates C code to be flashed to the low-power microcontroller that controls the fingertip sensors. This compiler allows for a lightweight and easy-to-integrate set of code. When profiled, the *nn4mc*-generated code achieves an average of 32.8 ms to perform each forward pass, which fits properly with the overall 16 Hz sampling frequency of the rest of the firmware at the embedded platform.

RESULTS

Figures 4a shows the raw barometric response of the sensor to an applied load. Figure 4b shows real-time results for force prediction in Newtons. From this data, we compute a root mean squared error of 1.38 N and mean absolute error of 0.68 N. Figure 4c shows the offline testing set region detection error. Regions 4 and 6 yield the maximum error with a failure rate of 6% and Region 3 yields the minimum error with a failure rate of 0%. For the probability of the location of contact, we truncate values above 50% as a positive contact prediction and values below 50% as a negative contact prediction.

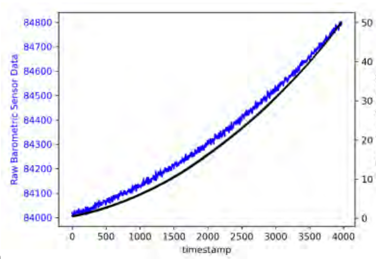

(a)

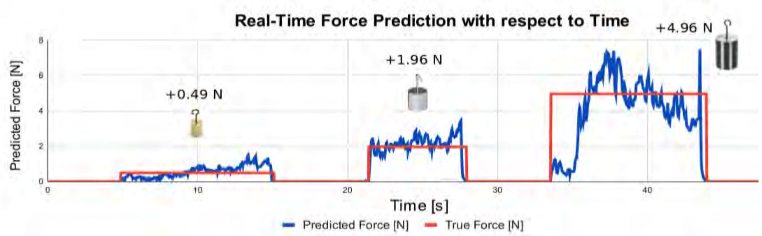

(b)

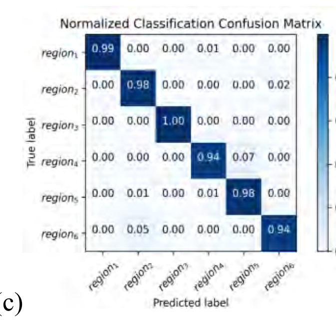

(c)

Figure 4: (a) Raw barometric signal after applied load. (b) Real-time onboard force prediction results using three dead weights. (c) Confusion matrix representing offline classification performance.

DISCUSSION

Figure 4a shows the raw barometric sensor responding to changes in the applied pressure prior to the predictions made by the neural network. Figure 4b shows the predictions for force to have an average absolute error of 0.68 Newtons, which comes mostly from the transient response to the finger being exposed to a 500-gram weight and human error when placing this weight. If we scale this error to the maximum force tested in the experiment illustrated in this figure, we obtain an approximate of 13.6%, which exceeds the allowable tolerance of less than 5% of error in the force prediction. These results can be improved by refining the data collection experiment.

For the contact localization, we observe that the regions located at the distal half of the fingertip yield the highest performing predictions. This corresponds to the actual location of the sensors on the PCB, as shown in Figure 1b. In the future, we wish to test whether this data is sufficient for a semi-autonomous control paradigm for prosthetic hands, which will inform how to further improve the proposed design and machine learning architecture.

CONCLUSION

We demonstrated measuring force and proximity measurements within a commercially available prosthetic finger. We used an embedded, real-time neural network to predict force values and classify where the forces are imparted on the fingertip sensor. The combination of force, proximity, and spatial location data in an onboard embedded processor provide an opportunity for real-time control of prosthetic devices in a new fashion, in particular sharing control of a myoelectric prosthetic hand between the prosthetic user and the robotic device. Future work will implement a three-phased myoelectric control system followed by testing with able-bodied subjects and amputees.

ACKNOWLEDGEMENTS

We'd like to thank Rachel Sharpe for the assistance using the Instron UTM machine at the Integrated Teaching and Learning Laboratory (ITLL). We'd like to thank the Air Force Office of Scientific Research (Grant No. 83875-11094) and the National Institute of Biomedical Imaging And Bioengineering of the National Institutes of Health Award Number (Grant No. R41EB032723). We'd also like to thank the entire *nn4mc* development team at CU Boulder.

REFERENCES

[1] K. Ziegler-Graham, E. J. MacKenzie, P. L. Ephraim, T. G. Travison, and R. Brookmeyer, "Estimating the prevalence of limb loss in the United States: 2005 to 2050.," *Archives of physical medicine and rehabilitation*, vol. 89, no. 3, pp. 422–9, Mar. 2008, doi: 10.1016/j.apmr.2007.11.005.

[2] J. T. Belter, J. L. Segil, A. M. Dollar, and R. F. Weir, "Mechanical design and performance specifications of anthropomorphic prosthetic hands: a review," *Journal of rehabilitation research and development*, vol. 50, no. 5, pp. 599–618, Aug. 2013.

[3] P. D. Marasco, K. Kim, J. E. Colgate, M. A. Peshkin, and T. A. Kuiken, "Robotic touch shifts perception of embodiment to a prosthesis in targeted reinnervation amputees," *Brain*, vol. 134, no. 3, pp. 747–758, Mar. 2011, doi: 10.1093/brain/awq361.

[4] A. L. Edwards *et al.*, "Application of real-time machine learning to myoelectric prosthesis control: A case series in adaptive switching," *Prosthetics and orthotics international*, vol. 40, no. 5, pp. 573–581, 2016.

[5] S. Došen, C. Cipriani, M. Kostić, M. Controzzi, M. C. Carrozza, and D. B. Popović, "Cognitive vision system for control of dexterous prosthetic hands: experimental evaluation," *Journal of neuroengineering and rehabilitation*, vol. 7, no. 1, pp. 1–14, 2010.

[6] K. Z. Zhuang *et al.*, "Shared human–robot proportional control of a dexterous myoelectric prosthesis," *Nature Machine Intelligence*, vol. 1, no. 9, pp. 400–411, 2019.

[7] G. Puchhammer, "The tactile slip sensor: Integration of a miniaturized sensory device on an myoelectric hand," *Orthopadie-Technik Quarterly*, vol. 1, no. 2000, pp. 7–12, 2000.

[8] E. D. Engeberg and S. G. Meek, "Adaptive sliding mode control for prosthetic hands to simultaneously prevent slip and minimize deformation of grasped objects," *IEEE/ASME Transactions on Mechatronics*, vol. 18, no. 1, pp. 376–385, 2011.

[9] J. S. Hebert *et al.*, "Quantitative eye gaze and movement differences in visuomotor adaptations to varying task demands among upper-extremity prosthesis users," *JAMA network open*, vol. 2, no. 9, pp. e1911197–e1911197, 2019.

[10] D. W. Tan, M. A. Schiefer, M. W. Keith, J. R. Anderson, J. Tyler, and D. J. Tyler, "A neural interface provides long-term stable natural touch perception," *Science Translational Medicine*, vol. 6, no. 257, pp. 257ra138-257ra138, Oct. 2014, doi: 10.1126/scitranslmed.3008669.

[11] S. A. Manzano, D. Hughes, C. Simpson, R. Patel, and N. Correll, "Embedded neural networks for robot autonomy," *arXiv preprint arXiv:1911.03848*, 2019.

[12] J. Segil, R. Patel, J. Klingner, R. F. ff Weir, and N. Correll, "Multi-modal prosthetic fingertip sensor with proximity, contact, and force localization capabilities," *Advances in Mechanical Engineering*, vol. 11, no. 4, p. 1687814019844643, 2019.

[13] J. Chung, C. Gulcehre, K. Cho, and Y. Bengio, "Empirical evaluation of gated recurrent neural networks on sequence modeling," *arXiv preprint arXiv:1412.3555*, 2014.